Biogeosciences, 12, 2247–2259, 2015
www.biogeosciences.net/12/2247/2015/
doi:10.5194/bg-12-2247-2015

Biogeosciences Open Access

Effects of CO_2 and iron availability on *rbcL* gene expression in Bering Sea diatoms

H. Endo[1,2], K. Sugie[1,3,4], T. Yoshimura[3], and K. Suzuki[1,2]

[1]Faculty of Environmental Earth Science/Graduate School of Environmental Science, Hokkaido University, North 10 West 5, Kita-ku, Sapporo, Hokkaido 060-0810, Japan
[2]CREST, Japan Science and Technology, North 10 West 5, Kita-ku, Sapporo, Hokkaido 060-0810, Japan
[3]Central Research Institute of Electric Power Industry, 1646 Abiko, Abiko, Chiba 270-1194, Japan
[4]Research Institute for Global Change, Japan Agency for Marine-Earth Science and Technology (JAMSTEC), 3173-25 Showa-machi, Kawasaki-ku, Yokohama, Kanagawa 236-0001, Japan

Correspondence to: H. Endo (endo@ees.hokudai.ac.jp)

Received: 6 November 2014 – Published in Biogeosciences Discuss.: 20 December 2014
Revised: 26 February 2015 – Accepted: 22 March 2015 – Published: 15 April 2015

Abstract. Iron (Fe) can limit phytoplankton productivity in approximately 40 % of the global ocean, including in high-nutrient, low-chlorophyll (HNLC) waters. However, there is little information available on the impact of CO_2-induced seawater acidification on natural phytoplankton assemblages in HNLC regions. We therefore conducted an on-deck experiment manipulating CO_2 and Fe using Fe-deficient Bering Sea water during the summer of 2009. The concentrations of CO_2 in the incubation bottles were set at 380 and 600 ppm in the non-Fe-added (control) bottles and 180, 380, 600, and 1000 ppm in the Fe-added bottles. The phytoplankton assemblages were primarily composed of diatoms followed by haptophytes in all incubation bottles as estimated by pigment signatures throughout the 5-day (control) or 6-day (Fe-added treatment) incubation period. At the end of incubation, the relative contribution of diatoms to chlorophyll *a* biomass was significantly higher in the 380 ppm CO_2 treatment than in the 600 ppm treatment in the controls, whereas minimal changes were found in the Fe-added treatments. These results indicate that, under Fe-deficient conditions, the growth of diatoms could be negatively affected by the increase in CO_2 availability. To further support this finding, we estimated the expression and phylogeny of *rbcL* (which encodes the large subunit of RuBisCO) mRNA in diatoms by quantitative reverse transcription polymerase chain reaction (PCR) and clone library techniques, respectively. Interestingly, regardless of Fe availability, the transcript abundance of *rbcL* decreased in the high CO_2 treatments (600 and 1000 ppm). The present study suggests that the projected future increase in seawater pCO_2 could reduce the RuBisCO transcription of diatoms, resulting in a decrease in primary productivity and a shift in the food web structure of the Bering Sea.

1 Introduction

The atmospheric CO_2 concentration has risen from a pre-industrial level of approximately 280 ppm to the present level of approximately 400 ppm (WMO, 2013). Since the Industrial Revolution, the ocean has absorbed about one-third of CO_2 emitted by human activity (Sabine et al., 2004). It is predicted that the atmospheric CO_2 concentration could reach more than 700 ppm by the end of the 21st century (Meehl et al., 2007), driving a surface seawater pH decrease of 0.3–0.4, ocean acidification (Caldeira and Wickett, 2003). Such a rapid decrease in seawater pH has most likely not occurred for at least millions of years in the Earth's history (Pearson and Palmer, 2000). Therefore, it has been suggested that these predicted changes in seawater carbonate chemistry would have enormous impacts on the health and function of marine organisms (Raven et al., 2005).

In the last decade, numerous studies have been performed to evaluate the impacts of ocean acidification on marine phytoplankton. In laboratory incubation experiments using individual species (a single strain), the response of phytoplankton to increased CO_2 levels differed among phytoplankton

species, possibly depending on their ability to assimilate carbon (Riebesell and Tortell, 2011; Collins et al., 2014). In the natural environment, these taxon-specific differences in CO_2 response can cause a shift in the phytoplankton community composition (Engel et al., 2008; Meakin and Wyman, 2011; Endo et al., 2013) and subsequent changes in ocean trophic structures and biogeochemical cycles (Riebesell et al., 2007; Yoshimura et al., 2013). However, the current understanding of the effects of elevated CO_2 on marine phytoplankton is still insufficient at the community level.

In terms of physiology, CO_2 is fixed by the carboxylation enzyme ribulose bisphosphate carboxylase / oxygenase (RuBisCO) in the Calvin–Benson–Bassham (CBB) cycle. In general, the half-saturation constant of the enzyme ranges between 20 and 70 µmol kg^{-1} CO_2 (Badger et al., 1998), whereas the ambient seawater CO_2 levels are between 10 and 25 µmol kg^{-1}. Therefore, the present CO_2 concentration could be insufficient to ensure effective RuBisCO carboxylation. The progression of ocean acidification could enhance photosynthetic carbon fixation in marine phytoplankton by increasing CO_2 availability.

Recent advances in molecular biology techniques have enabled us to examine the taxon-specific responses to environmental changes by quantifying functional gene expression in natural phytoplankton assemblages. For example, John et al. (2007a) developed a suite of quantitative reverse transcription polymerase chain reaction (qRT-PCR) assays to quantify *rbcL* (gene encoding the large subunit of RuBisCO) mRNA in *Synechococcus*, haptophytes, and heterokonts including diatoms. John et al. (2007b) demonstrated a strong negative correlation between diatom-specific *rbcL* mRNA abundance and seawater pCO_2 in the Mississippi River plume, suggesting that diatoms were responsible for the greatest drawdown in seawater pCO_2. In addition, positive correlations between diatom-specific *rbcL* transcripts and light-saturated photosynthetic rates (P_{max}) in seawater were reported (Corredor et al., 2004; John et al., 2007b). These results suggest that *rbcL* expression in diatoms could be used to estimate the photosynthetic carbon-fixation capacity of natural phytoplankton assemblages. Therefore, quantification of clade-specific *rbcL* transcripts can be used to assess the physiological photosynthetic responses of individual phytoplankton taxa to environmental changes.

The oceanic Bering Sea investigated in this study is a high-nutrient, low-chlorophyll (HNLC) region (Banse and English, 1999), where low iron (Fe) availability limits phytoplankton growth and nitrate utilization, so surface chlorophyll *a* (Chl *a*) concentrations usually remain low in the summer (Suzuki et al., 2002). Despite the low phytoplankton biomass, the oceanic domain has the greatest amount of total primary and secondary production in the Bering Sea (Springer et al., 1996). Suzuki et al. (2002) reported that diatoms were the dominant phytoplankton group in the oceanic regions of the Bering Sea in the summer. In addition, Takahashi et al. (2002) showed that diatoms had the greatest contribution in the sinking particles in the area. However, less is known about the combined effects of ocean acidification and Fe enrichment on diatoms in such HNLC regions. In addition, there are no reports on the effects of CO_2 and Fe availability on *rbcL* transcription of natural diatom community in HNLC regions.

The purpose of this study is to clarify the responses of phytoplankton, especially diatoms, to CO_2 enrichment under Fe-depleted and Fe-replete conditions in the Bering Sea basin using on-deck bottle incubation. Recently, Sugie et al. (2013) reported changes in phytoplankton biomass and nutrient stoichiometry in this experiment. They showed that Chl *a* biomass decreased with increased CO_2 levels only in Fe-depleted treatments, suggesting that Fe deficiency and increased CO_2 synergistically reduced the growth of phytoplankton in the study area. In addition, Yoshimura et al. (2014) demonstrated that the net production of particulate organic carbon (POC) and total organic carbon (TOC) decreased under high CO_2 levels only in the Fe-limited treatments, whereas those in the Fe-replete treatments were insignificantly different. These studies suggest that the increase in CO_2 could have negative impacts on phytoplankton growth and/or organic-matter production especially under Fe-depleted conditions. However, the molecular mechanisms of photosynthetic carbon assimilation in phytoplankton assemblages were not mentioned in the previous studies. Therefore, in the present paper, we primarily focused on changes in *rbcL* transcripts in diatoms with different CO_2 and/or Fe availability.

2 Materials and methods

2.1 Experimental setup

The study was carried out aboard the R/V *Hakuho Maru* (JAMSTEC) during the KH-09-4 cruise in September 2009. The water samples for incubation were collected from 10 m depth at a station (53°05′ N, 177°00′ W) in the Bering Sea on 9 September with acid-cleaned Niskin-X bottles attached to a conductivity–temperature–depth carousel multisampling system (CTD-CMS) system. A total of 300 L of seawater was poured into six 50 L polypropylene carboys through acid-clean silicon tubing with a 197 µm mesh Teflon net to remove large particles. Subsamples were taken from each carboy and poured into triplicate acid-cleaned 12 L polycarbonate bottles (18 bottles total) for incubation. Initial samples were collected from each carboy. All sampling was carried out using a trace-metal clean technique to avoid any trace metal contamination. Prior to incubation, $FeCl_3$ solutions (5 nmol L^{-1} in final concentration) were added to 12 bottles in order to reduce Fe limitation for the phytoplankton communities. The CO_2 levels in the incubation bottles were manipulated by injecting CO_2-controlled dry air purchased from a commercial gas supply company (Nissan-Tanaka Co., Japan). The air

mixtures were passed through 47 mm PTFE filters (0.2 µm pore size, Millipore) before being added to the incubation bottles. The detailed procedures for trace metal clean techniques were described in Yoshimura et al. (2013). The CO_2 concentrations were set at 380 and 600 ppm for the non-Fe-added (control) bottles (hereafter referred to as "C-380" and "C-600", respectively), and 180, 380, 600, and 1000 ppm for the Fe-added bottles (hereafter referred to as "Fe-180", "Fe-380", "Fe-600", and "Fe-1000", respectively). Incubation was performed on deck in temperature-controlled water-circulating tanks for 5 days (control) or 6 days (Fe-added treatment) at the in situ temperature (8.2 °C) and 50 % surface irradiance adjusted by natural density screens. The sampling opportunities for each parameter are shown in Table S1 in the Supplement.

2.2 Carbonate chemistry, nutrients, and Chl *a*

The detailed methodology and basic chemical and biological parameters were reported in Sugie et al. (2013). In brief, during the incubation experiment, samples were collected from the incubation bottles for dissolved inorganic carbon (DIC), total alkalinity (TA), nutrients, and Chl *a* determination. DIC and TA concentrations were measured with a total alkalinity analyzer using the potentiometric Gran plot method (Kimoto Electric) following Edmond (1970). The levels of pCO_2 and pH were calculated from the DIC and TA using the CO2SYS program (Lewis and Wallance, 1998). Concentrations of nitrate plus nitrite, nitrite, phosphate, and silicic acid were measured using a QuAATro-2 continuous-flow analyzer (Bran+Luebbe). The concentration of total dissolved Fe (TD-Fe) was determined by a flow-injection method with chemiluminescence detection (Obata et al., 1993). Chl *a* concentrations were determined with a Turner Design fluorometer (model 10-AU) with the non-acidification method (Welschmeyer, 1994).

2.3 HPLC and CHEMTAX analyses

Samples for high-performance liquid chromatography (HPLC) pigment analysis were collected on days 3 and 5 for the control treatments and on days 2, 4, and 6 for the Fe-added treatments. Water samples (400–1000 mL) were filtered onto GF/F filters under gentle vacuum (< 0.013 MPa) and stored in liquid nitrogen or a deep freezer (−80 °C) until analysis. HPLC pigment analysis was performed following the method of Endo et al. (2013).

To estimate the temporal changes in phytoplankton community structure during incubation, the CHEMTAX program (MacKey et al., 1996) was used following Endo et al. (2013). Briefly, optimal initial ratios were obtained following the method of Latasa (2007). Matrix **A** was obtained from Suzuki et al. (2002) (Table S2), who examined phytoplankton community compositions in the Bering Sea. Matrices **B**, **C**, and **D** were also prepared to determine the optimal pigment / Chl *a* ratios (Table S2). The pigment ratios of Matrices **B** and **C** were double and half the Matrix **A** ratio, respectively. For Matrix **D**, values of 0.75, 0.5, and 0.25 for dominant (rank according to high pigment / Chl *a* ratio: 1–5), secondary (rank 6–10), and minor (rank 11–15) pigments, respectively, were multiplied by each pigment ratio of Matrix **A**. We averaged the successive convergent ratios after the 10 runs among the 4 matrices to identify the most promising initial pigment ratios. The calculated final pigment / Chl *a* ratios in both the control and Fe-added treatments (Table S3) were within the range of values reported in Mackey et al. (1996), Wright and van den Enden (2000), and Suzuki et al. (2002).

2.4 qPCR and qRT-PCR

Water samples for DNA and RNA analyses were collected on days 3 and 5 for the control treatments and on days 2, 4, and 6 for the Fe-added treatments. DNA samples (400–500 mL) were collected onto 25 mm, 0.2 µm pore size polycarbonate Nuclepore filters (Whatman) with gentle vacuum (< 0.013 MPa) and stored in liquid nitrogen or a deep freezer at −80 °C until analysis. DNA extraction was performed following the method of Endo et al. (2013). Extracted DNA pellets were resuspended in 100 µL of 10 mM Tris-HCl buffer (pH 8.5).

For RNA analysis, seawater samples (400–500 mL) were filtered onto 25 mm, 0.2 µm pore size polycarbonate Nuclepore filters (Whatman) with gentle vacuum (< 0.013 MPa) and stored in 1.5 mL cryotubes previously filled with 0.2 g of muffled 0.1 mm glass beads and 600 µL RLT buffer (Qiagen) with 10 µL mL^{-1} β-mercaptoethanol (Sigma, St. Louis, USA). RNA samples were stored in liquid nitrogen or a deep freezer at −80 °C until analysis. Extraction and purification of RNA samples were performed using the RNeasy extraction kit (Qiagen) on a vacuum manifold with on-column DNA digestion using RNase-free DNase (Qiagen) according to the manufacturer's protocol. RNA was eluted using 50 µL of RNase-free H_2O. Total RNA was then reverse transcribed into complementary DNA (cDNA) using the PrimeScript™ RT regent Kit with gDNA Eraser (Takara) following the manufacturer's specifications.

Following Smith et al. (2006), we used double-stranded DNA and single-stranded cDNA standards for DNA and cDNA quantification, respectively. Standard curves for *rbcL* DNA were generated from plasmid DNA (pUC18, Takara) containing an artificial gene fragment (113 bp in size) of *rbcL* from the diatom *Thalassiosira weissflogii* (CCMP1336). The plasmid DNA was linearized with *Hind*III (Takara) and quantified using a Thermo NanoDrop spectrophotometer (ND-1000). On the other hand, to produce the cDNA standard, a PCR-amplified *rbcL* gene fragment of *T. weissflogii* (CCMP1336) was inserted into a plasmid DNA (pCR2.1, Invitrogen). The plasmid DNA was purified using the Plasmid maxi kit (Qiagen) and linearized with *Bam*HI (Takara),

and in vitro transcription was performed using T7 RNA polymerase (Invitrogen) for 2 h at 37 °C with Recombinant RNase Inhibitor (Takara). To eliminate DNA contamination, RNA was digested for 2 min at 42 °C using gDNA Eraser (Takara). RNA was purified using an RNeasy column (Qiagen) following the manufacturer's instructions and quantified with a Ribogreen RNA quantification kit (Molecular Probes) using the manufacturer's standard. RNA was reverse transcribed into cDNA using the PrimeScript™ RT regent Kit with gDNA Eraser (Takara).

Copy numbers of DNA and cDNA standards were calculated using the equation of Smith et al. (2006), where the molecular mass of each nucleotide (or nucleotide pair) in double- and single-stranded DNA is assumed to be 660 and 330 Da, respectively. Serial dilutions of DNA and cDNA standards were prepared using sterilized Milli-Q water.

To amplify the *rbcL* gene and cDNA fragments from diatoms, the following specific primer set designed by John et al. (2007a) was used:

Forward primer: 5′-GATGATGARAAYATTAACTC-3′
Reverse primer: 5′-TAWGAACCTTTWACTTCWCC-3′.

Real-time PCR amplification was performed using SYBR Premix Ex Taq II (Perfect Real Time, Takara) with primer concentrations of 0.4 µM each and a Thermal Cycler Dice Real Time System (TP800, Takara). Diluted nucleic acid standards were then added to the PCR mixture. The thermal cycling conditions were 95 °C for 60 s, then 40 cycles of 95 °C for 5 s, and 52 °C for 60 s. The fluorescence intensity of the complex formed by SYBR green and the double-stranded PCR product was continuously monitored from cycle 1 to 40. Quantification was achieved by the second-derivative maximum method (Luu-The et al., 2005), and the copy number for each sample was determined by the standard curves generated by serial dilutions of the standards.

2.5 Clone libraries

Clone libraries of *rbcL* cDNA were constructed for the C-380 and C-600 samples on day 3, and Fe-380 and Fe-600 samples on day 2. The cDNA samples were PCR amplified with the diatom-specific primer set and thermal cycling conditions described above using the Takara Ex Taq Hot Start Version (Takara). Triplicate PCR products were mixed and then purified with agarose gel electrophoresis and the PureLink Quick Gel Extraction Kit (Invitrogen). Purified amplicons from cDNA samples were then cloned into the pCR2.1 vector using the TOPO TA cloning kit (Invitrogen) following the manufacturer's instructions. Thirty-five to 50 colonies were randomly picked from each clone library. Correct cDNA insertions were identified by PCR amplification using the M13 forward (5′-GTAAAACGACGGCCAG-3′) and reverse (5′-CAGGAAACAGCTATGA-3′) primers flanking the cloning site. Plasmid DNA containing the inserts was cycle-sequenced using the Big Dye Terminator v3.1 Kit (Applied Biosystems) with the M13 forward primer. The cycle sequencing products were cleaned by isopropanol precipitation. Sequencing was performed with a 3130 Genetic Analyzer (Life Technologies). The obtained sequences were compared with *rbcL* sequences deposited in GenBank database (http://www.ncbi.nlm.nih.gov) using the Basic Local Alignment Search Tool (BLAST) query engine. Our *rbcL* cDNA sequences were deposited in the DNA Data Bank of Japan (DDBJ) with the following accession numbers AB985799–AB986033.

2.6 Phylogenetic and diversity analyses

The *rbcL* sequences obtained were assembled into operational taxonomic units (OTUs) with > 95 % sequence identity, and rarefaction curves were plotted for each clone library with the software mothur v. 1.27 (Schloss et al., 2009). To estimate OTU richness, chao1 index (Chao, 1984) values were calculated using the number of singleton sequences obtained in this study. Genetic diversity was assessed based on the Shannon–Wiener index (H', Shannon, 1948) and Simpson's index (D, Simpson, 1949). The statistical significance of differences in the compositions of pairs of *rbcL* sequences in the libraries was tested using LIBSHUFF (Singleton et al., 2001). The LIBSHUFF program determined the integral form of the Cramer–von Mises statistic for each pair of communities using 10 000 randomizations. Any two libraries were considered to be significantly different from each other if the lower of the significance values generated by the software was < 0.025 ($p < 0.05$).

2.7 Statistical analysis

Statistical analyses were performed with the program R (http://www.r-project.org). To assess the statistically significant differences between pCO_2 levels in the control treatments or between control and Fe treatments, Welch's t test was used. Differences among pCO_2 levels in the Fe-added treatments were evaluated with Kruskal–Wallis one-way analysis of variance (ANOVA). Holm's test for multiple comparisons was used to identify the source of the variance. For all of the analyses, the confidence level was set at 95 % ($p < 0.05$).

3 Results

3.1 Experimental conditions

The bubbling of CO_2-controlled air succeeded in creating significant gradients in pCO_2, pH, and DIC in the different CO_2 treatments except on day 4 in the Fe-added treatments, when those values did not significantly differ between Fe-380 and Fe-600 (Table 1; Fig. S1 in the Supplement). The initial concentrations of nitrate, phosphate, and silicic acid

Table 1. Carbonate chemistry, nutrients, and Fe parameters (value ± 1 standard deviation, $n = 3$) during the incubation experiment. Carbonate parameters are the initial and mean values throughout the incubation. Macronutrients and Fe parameters are the values at the initial or final sampling days (i.e., day 5 for the control and day 6 for the Fe-added treatments). Standard deviation was not assessed for initial TD-Fe concentration because samples were collected from single source. See Figs. S1 and S2 for the complete data set.

	DIC ($\mu mol\,kg^{-1}$)	TA ($\mu mol\,kg^{-1}$)	pCO_2 (µatm)	CO_2 ($\mu mol\,kg^{-1}$)	pH (total scale)
C-Initial	2086.4 ± 2.8	2249.1 ± 5.0	388.4 ± 18.1	18.4 ± 0.9	8.05 ± 0.02
C-380	2075.5 ± 8.1	2252.9 ± 10.8	355.7 ± 34.7	16.8 ± 1.6	8.09 ± 0.04
C-600	2151.6 ± 7.8	2250.9 ± 4.7	604.1 ± 36.2	28.5 ± 1.7	7.88 ± 0.02
Fe-Initial	2085.3 ± 0.8	2250.0 ± 4.9	383.4 ± 12.6	18.1 ± 0.6	8.06 ± 0.01
Fe-180	1959.9 ± 62.0	2244.1 ± 16.0	202.0 ± 50.9	9.5 ± 2.4	8.21 ± 0.10
Fe-380	2068.5 ± 27.7	2235.7 ± 14.9	375.9 ± 47.9	17.8 ± 2.3	8.01 ± 0.05
Fe-600	2120.6 ± 33.5	2248.5 ± 12.0	512.6 ± 135.5	24.2 ± 6.4	7.96 ± 0.11
Fe-1000	2200.2 ± 12.6	2248.4 ± 9.8	913.8 ± 159.8	43.2 ± 7.6	7.72 ± 0.07

	Nitrate ($\mu mol\,L^{-1}$)	Phosphate ($\mu mol\,L^{-1}$)	Silicic acid ($\mu mol\,L^{-1}$)	TD-Fe ($nmol\,L^{-1}$)
C-Initial	18.06 ± 0.10	1.47 ± 0.01	16.95 ± 0.12	1.35
C-380	7.09 ± 0.27	0.65 ± 0.02	0.28 ± 0.05	0.27 ± 0.03
C-600	12.01 ± 0.27	0.98 ± 0.02	3.04 ± 0.32	0.29 ± 0.04
Fe-Initial	18.09 ± 0.11	1.47 ± 0.01	16.90 ± 0.12	5.50 ± 0.10
Fe-180	0.13 ± 0.04	0.10 ± 0.01	0.66 ± 0.09	4.60 ± 0.19
Fe-380	0.09 ± 0.00	0.12 ± 0.04	0.50 ± 0.01	4.48 ± 0.12
Fe-600	0.08 ± 0.00	0.10 ± 0.00	0.50 ± 0.01	4.34 ± 0.08
Fe-1000	0.08 ± 0.00	0.08 ± 0.02	0.47 ± 0.02	4.18 ± 0.24

were 18.06 ± 0.10, 1.47 ± 0.01, and 16.90 ± 0.12 µmol L^{-1}, respectively (Table 1). In the control bottles, these macronutrients remained until the end of the incubation in both CO_2 treatments except for silicic acid, which was almost depleted on day 5 in the C-380 treatment (Fig. S2). In the Fe-added bottles, macronutrients were depleted on days 4 or 5 in all CO_2 treatments (Fig. S2). The TD-Fe concentration was 1.35 nmol L^{-1} in the initial seawater, and it remained low throughout the experiment in the control treatments (Table 1). In the Fe-added treatments, the TD-Fe concentrations were 5.50 ± 0.10 nmol L^{-1} in the initial bottles and remained above 4 nmol L^{-1} until the end of incubation (Table 1). The initial Chl *a* concentration was 1.96 ± 0.14 µg L^{-1} (Table 1). In the control bottles, the Chl *a* concentration increased until the end of the incubation and reached 10.22 ± 0.89 µg L^{-1} in the C-380 and 6.28 ± 0.64 µg L^{-1} in the C-600 treatments (Fig. S3). In the Fe-added bottles, the Chl *a* concentration increased rapidly and reached the maximum on day 4 in the Fe-180 and Fe-380 treatments (27.51 ± 0.71 and 28.45 ± 3.40 µg L^{-1}, respectively), on day 5 in the Fe-600 and Fe-1000 treatments (27.68 ± 0.44 and 27.32 ± 3.05 µg L^{-1}, respectively), and then declined toward the end of the incubation (Fig. S3).

3.2 Phytoplankton pigments

Throughout the experiment, the concentrations of fucoxanthin (Fuco), mainly a biomarker for diatoms (Ondrusek et al., 1991; Suzuki et al., 2011), and 19′-hexanoyloxyfucoxanthin (19′-Hex), an indicator of haptophytes (Jeffrey and Wright, 1994), were relatively high among the phytoplankton pigments. In the control bottles, the concentrations of Fuco and 19′-Hex increased over time and reached the maximum values on day 5 in both the C-380 and C-600 treatments (Fig. 1a and c). After day 3, the concentrations of Fuco and 19′-Hex were higher in the C-380 treatment than in the C-600 treatment (day 5: Welch's t test C-380 > C-600, $p < 0.05$), although no statistical significance was assessed on day 3 because samples were collected from each single bottle. In the Fe-added bottles, Fuco concentrations increased throughout the incubation and reached the maximum values on day 6, whereas 19′-Hex concentrations decreased after day 4 (Fig. 1b and d). The concentrations of Fuco were significantly different among CO_2 treatments on day 6 (Kruskal–Wallis ANOVA, $p < 0.05$), although these differences were not supported by multiple comparisons (Holm's test, $p > 0.05$). Significant differences among CO_2 treatments were also found for the 19′-Hex concentration on day 6 (Kruskal–Wallis ANOVA, $p < 0.05$), and the values in the Fe-180 treatment was significantly higher than those in the Fe-1000 treatment (Holm's test, $p < 0.05$).

3.3 CHEMTAX outputs

In the initial phytoplankton community, diatoms and haptophytes were the predominant numbers of the phytoplankton

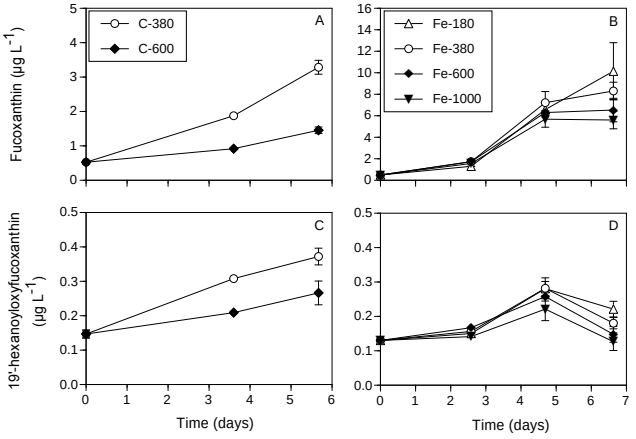

Figure 1. Temporal changes in fucoxanthin **(a, b)** and 19′-hexanoyloxyfucoxanthin **(c, d)** concentrations. Graphs on the left and right sides indicate data from the control and Fe-added treatments, respectively. Error bars denote ± 1 standard deviation (SD, $n = 3$). Standard deviations were not assessed on days 2 (Fe-added treatments) and 3 (control treatments) because samples were collected from each single bottle.

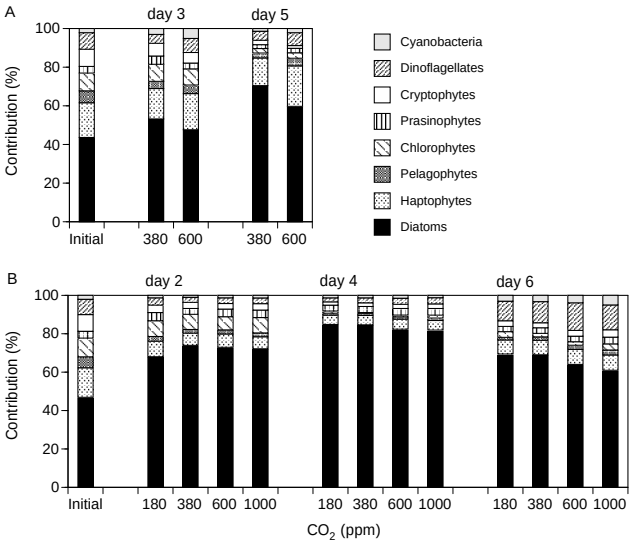

Figure 2. Mean contributions of each phytoplankton group to total Chl *a* biomass estimated by CHEMTAX in the **(a)** control bottles at 380 and 600 ppm CO_2, and **(b)** Fe-added bottles at 180, 380, 600, and 1000 ppm CO_2 ($n = 1$ or 3).

groups (i.e., they contributed 45 and 17 % of the Chl *a* concentration, respectively). The initial contributions of chlorophytes, cryptophytes, peridinin-containing dinoflagellates, pelagophytes, prasinophytes, and cyanobacteria to the Chl *a* biomass were 10, 9, 8, 5, 4, and 2 %, respectively. In the control bottles, the contributions of diatoms to the Chl *a* biomass increased with time, and their contributions reached the maximum (70 % at the C-380 and 60 % at the C-600 treatments) on day 5 (Fig. 2a). On day 5, the contribution of diatoms in the C-380 treatment was significantly higher than that in the C-600 treatment (Welch's *t* test, $p < 0.05$). However, the contribution of haptophytes to the Chl *a* biomass was higher in the C-600 treatment (21 %) than in the C-380 treatment (14 %) on day 5 (Welch's *t* test, $p < 0.05$). Increases in the contributions of diatoms were also observed in the Fe-added treatment, and the contributions reached the maximum (82–85 %) on day 4 in all CO_2 treatments (Fig. 2b). In terms of diatom contribution, a significant difference among CO_2 treatments was not detected with Kruskal–Wallis ANOVA ($p > 0.05$) in the Fe-added bottles. The contributions of haptophytes to Chl *a* biomass did not differ significantly among CO_2 levels in the Fe-added bottles (Kruskal–Wallis ANOVA, $p > 0.05$).

3.4 Expression of diatom *rbcL* gene

A significant linear relationship between the Fuco concentration and the diatom-specific *rbcL* gene copy number was found (regression analysis: $r^2 = 0.677$, $p < 0.001$, $n = 28$) in our experiment (Fig. 3). In the control bottles, the transcript abundance normalized to gene abundance (i.e., cDNA / DNA) of the diatom-specific *rbcL* gene fragment for

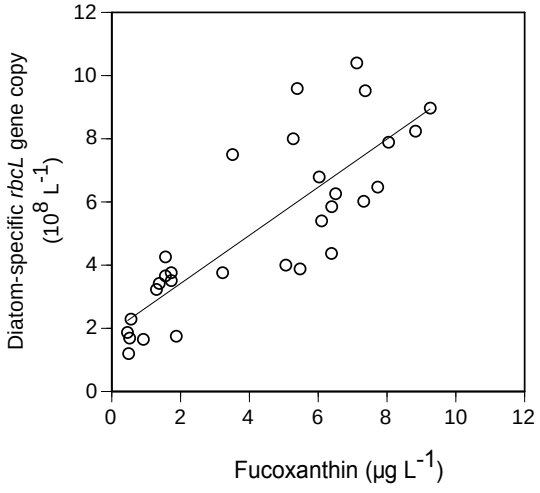

Figure 3. Relationship between fucoxanthin concentration and diatom-specific *rbcL* copy number ($y = 7.62 \times 10^8 x + 1.90 \times 10^8$, $r^2 = 0.677$, $p < 0.001$, $n = 28$).

the C-380 treatment was significantly higher than that of the C-600 treatment on day 3 (Fig. 4; Welch's *t* test, $p < 0.05$). In the Fe-added bottles, the cDNA / DNA ratio of the diatom *rbcL* fragment in the lower CO_2 treatments (Fe-180 and Fe-380) was higher than that in the Fe-600 treatment on day 2 (Fig. 4; Holm's test, $p < 0.05$).

3.5 Clone libraries of diatom *rbcL* cDNA

Rarefaction curves were plotted for the *rbcL* cDNA libraries (Fig. 5). In terms of unique taxa, the highest num-

Table 2. Number of OTUs, richness index, and diversity indices (value ± 95 % confidence interval) for *rbcL* cDNA libraries obtained from the initial seawater and the incubation bottles on day 2 (Fe-380 and Fe-600) and day 3 (C-380 and C-600).

Library	No. of sequences	No. of OTUs	Chao1	H'	D
Initial	35	10	25.0	1.81 ± 0.32	0.197 ± 0.086
C-380	50	15	20.0	1.98 ± 0.36	0.232 ± 0.110
C-600	50	14	29.0	1.60 ± 0.41	0.369 ± 0.148
Fe-380	50	13	23.0	2.24 ± 0.23	0.116 ± 0.042
Fe-600	50	12	19.5	2.01 ± 0.26	0.158 ± 0.053

ber of OTUs was found in the C-380 treatment (Table 2). The highest chao1 value was found in the C-600 treatment, whereas the lowest value was found in the Fe-600 treatment. Shannon–Wiener and Simpson diversity indices revealed that the cDNA libraries in the 380 ppm CO_2 bottles were more diverse than those in the 600 ppm CO_2 bottles in both the control and Fe-added treatments, although the values were not statistically significant between CO_2 treatments (*t* test, $p > 0.05$) (Table 2).

All sequences obtained from the cDNA libraries were more than 95 % similar to sequences deposited in the GenBank. These sequences could be classified into the following 11 phylogenetic groups: Chaetocerotaceae, Coscinodiscaceae, Cymatosiraceae, Stephanodiscaceae, Thalassiosiraceae, unidentified centrics, Bacillariaceae, Naviculaceae, Fragillariaceae, unidentified pennates, and other eukaryotes by comparison with known *rbcL* sequences from GenBank. Sequences that could not classified into a specific diatom family (e.g., closely related to two or more diatom families with same similarity score) were assigned as unidentified centrics or unidentified pennates. Other eukaryotes consisted of haptophytes, pelagophytes, dictyochophytes, dinoflagellates, and diatoms which could not be assigned to centrics and pennates. For all of the cDNA libraries, more than 88 % of *rbcL* sequences were most closely affiliated with those of cultured diatoms. In the initial cDNA library, the most abundant sequences were closely affiliated with the diatom family Bacillariaceae (46 %), followed by other eukaryotes and Cymatosiraceae (17 and 14 %, respectively) (Fig. 6). The contributions of other diatom groups were less than 6 % in the initial clone library. In the control bottles, the contributions of Coscinodiscaceae increased to 12–14 %, whereas those of Cymatosiraceae decreased to 4 %. In the Fe-added bottles, the contributions of Chaetocerotaceae and unidentified centrics to the total increased to more than 8 and 20 %, respectively. In contrast, the contributions of Bacillariaceae decreased below 24 % in both the Fe-380 and Fe-600 treatments.

Statistic analysis using LIBSHUFF revealed that the cDNA libraries in the control treatments were not significantly different from the initial sample regardless of the CO_2 level, whereas those in the Fe-added bottles differed significantly from the initial assemblage (LIBSHUFF, $p < 0.05$) (Table 3). No significant difference in the cDNA library was found between C-380 and C-600 treatments in the control bottles (LIBSHUFF, $p > 0.05$). However, a significant difference between the Fe-380 and Fe-600 treatments was detected in the Fe-added bottles (LIBSHUFF, $p < 0.05$). In addition, cDNA libraries in the Fe-added bottles differed significantly from those of the control bottles in both the Fe-380 and Fe-600 treatments (LIBSHUFF, $p < 0.05$).

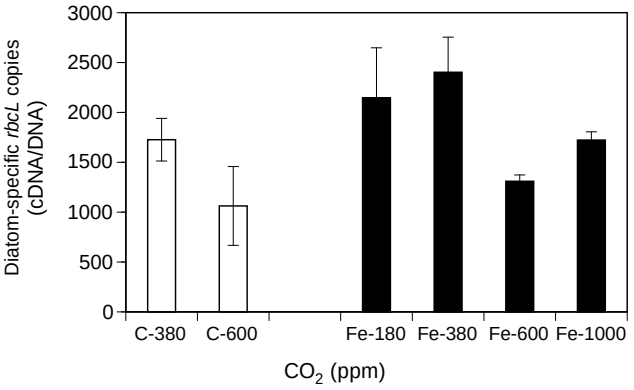

Figure 4. Abundances of *rbcL* mRNA (cDNA) normalized to *rbcL* gene copy number (*rbcL* cDNA / DNA) in the control bottles on day 3 and the Fe-added bottles on day 2. Open bars and closed bars denote control and Fe-added treatments, respectively. Error bars indicate ± 1 SD ($n = 3$).

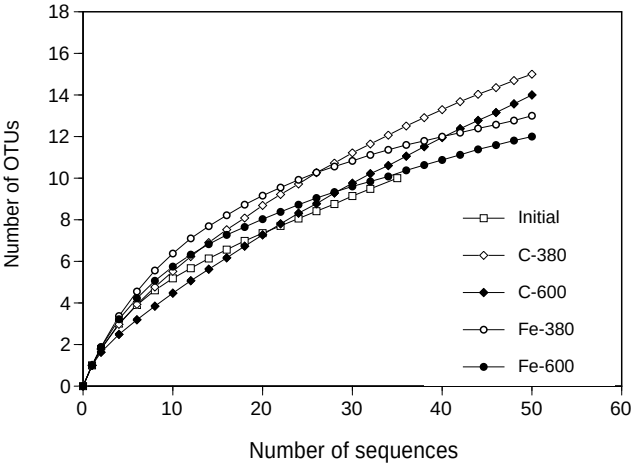

Figure 5. Rarefaction analysis of the diatom-specific *rbcL* clone libraries. The rarefaction curves, plotting the number of operational taxonomic units (OTUs) as a function of the number of sequences, were computed by the software mothur. C and Fe indicate the control and Fe-added treatments, respectively.

Table 3. Significance levels for differences among *rbcL* cDNA libraries as calculated with LIBSHUFF. p values < 0.05 are italicized.

		Library (Y)				
		Initial	C-380	C-600	Fe-380	Fe-600
Library (X)	Initial	–	0.434	0.573	0.383	0.587
	C-380	0.153	–	0.086	0.101	0.898
	C-600	0.523	0.500	–	*0.004*	0.033
	Fe-380	*< 0.001*	*< 0.001*	*< 0.001*	–	*0.002*
	Fe-600	*0.009*	*0.004*	*< 0.001*	0.030	–

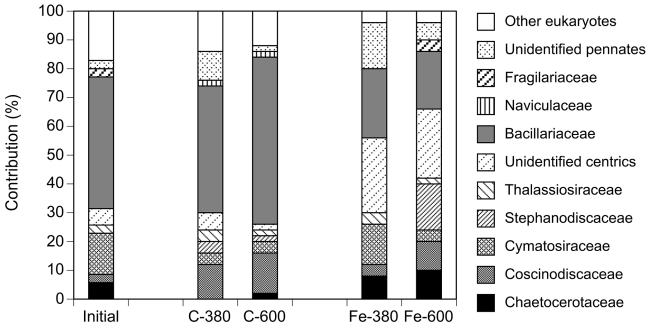

Figure 6. Relative phylotype contributions in the *rbcL* cDNA libraries obtained from the initial seawater and the incubation bottles at day 2 (Fe-380 and Fe-600) and day 3 (C-380 and C-600).

4 Discussion

4.1 Changes in phytoplankton community structure during incubation

Our CHEMTAX analysis suggested that the diatoms were the principal contributors to the Chl *a* biomass in the initial phytoplankton community, followed by haptophytes (Fig. 2). The results were consistent with those reported by Suzuki et al. (2002), who examined the community structure in the Bering Sea during the early summer of 1999. These results suggest that diatoms and haptophytes are ecologically important phytoplankton groups in the study area during the summer. Compared with previous reports in the area (Suzuki et al., 2002; Yoshimura et al., 2013), a relatively high initial Chl *a* concentration was observed in our experiment, possibly due to an intrusion of the coastal seawater mass from the Aleutian trenches (Sugie et al., 2013). However, the Fe infusion induced significant increases in Chl *a* biomass and concomitant rapid drawdowns of macronutrients in our incubation bottles (Fig. S2). This indicates that the seawater used for the incubation was Fe-limited for phytoplankton assemblages. Our HPLC and CHEMTAX results suggested that the increase in phytoplankton biomass was mainly due to an increase in diatoms (Figs. 1b and 2b).

We found that the growth of Fuco was less in the high CO_2 bottles in the control treatments (Fig. 1a), suggesting that the elevated CO_2 levels could have a negative impact on the diatom biomass in the study area. Negative effects on diatoms induced by an increase in CO_2 availability were also reported in field incubation experiments conducted in the Bering Sea and the Okhotsk Sea (Hare et al., 2007 and Yoshimura et al., 2010, respectively). However, such trends have rarely been observed in other regions of the world's oceans (e.g., Tortell et al., 2002; Kim et al., 2006; Feng et al., 2009; Hoppe et al., 2013; Endo et al., 2013). Therefore, the responses of phytoplankton assemblages to ocean acidification can differ among geographic locations due to the differences in the biogeography of phytoplankton and/or environmental conditions.

One possible cause of the geographic specificity in the open Bering Sea is the differences in the species composition of diatoms. Our microscope data showed that centric diatoms such as Chaetocerataceae and Rhizosoleniaceae were predominant at the beginning of the incubation in terms of carbon biomass, and the coastal diatom *Chaetoceros* spp. became predominant in all incubation bottles after day 2 (Sugie et al., 2013). Therefore, the relative decrease in Fuco biomass with increased CO_2 levels might be partially explained by the decrease in *Chaetoceros* spp. A previous field incubation experiment conducted in the Bering Sea also showed that the carbon biomass of the *Chaetoceros* spp. decreased at higher CO_2 levels (600–960 µatm CO_2), although it increased at 1190 µatm CO_2 (Yoshimura et al., 2013). However, Tortell et al. (2008) demonstrated that relative abundance of *Chaetoceros* spp. increased under elevated CO_2 levels in the Ross Sea. In the previous laboratory culture experiments, the effects of increased CO_2 on the growth and/or photosynthesis of *Chaetoceros* spp. were also inconsistent. For example, Ihnken et al. (2011) demonstrated that the growth of diatom *Chaetoceros muelleri* decreased with elevated CO_2 (decreased pH) levels although their photosynthetic capacity increased. In contrast, Trimborn et al. (2013) showed a significant increase in the growth rate of *Chaetoceros debilis* under high CO_2 conditions. In addition, no CO_2-related change in the growth and photosynthetic physiology of *Chaetoceros brevis* was found (Boelen et al., 2011). These results suggest that the responses to elevated CO_2 differ among *Chaetoceros* species.

The concentrations of 19′-Hex were significantly lower in the C-600 treatment than those in the C-380 treatment (Fig. 1c), suggesting that the ocean acidification could induce negative effects not only on the biomass of diatoms, but also on that of haptophytes in the study area. Similar results were obtained from the previous field studies in other regions (e.g., Feng et al., 2010; Endo et al., 2013). One possible factor underlying these decreases is the reduced carbonate-saturation states under high CO_2 conditions. The energetic cost of calcification in coccolithophores will increase with a decrease in pH (Mackinder et al., 2010). Therefore, additional energy might be needed for cell growth in seawater with high CO_2 levels. In addition, non-calcifying haptophytes such as

Phaeocystis spp. often dominate among haptophytes in the natural phytoplankton community (Schoemann et al., 2005), although the effects of ocean acidification on them are still not well understood. Therefore, additional study using a wide range of haptophyte species is required for a detailed understanding of the responses of the haptophyte community to CO_2-induced ocean acidification.

Our CHEMTAX outputs showed that the relative contributions of diatoms decreased with increased CO_2 levels, whereas the contributions of haptophytes increased in both the control and Fe-added bottles (Fig. 2). This indicates that the negative impacts of increased CO_2 on diatoms were greater than those on haptophytes and other phytoplankton groups. Another possibility is that competition between diatoms and other phytoplankton taxa could occur. For example, diatoms could become less competitive when silicic acid is exhausted because Si depletion significantly depressed growth and could induce their cell death (Harrison et al., 1977; Jiang et al., 2014). However, concentrations of silicic acid were not significantly different among CO_2 levels in the Fe-added treatments (Fig. S2f). Moreover, in the control treatments, silicic acid was almost depleted in the low CO_2 treatment after day 5 but not in the high CO_2 treatment (Fig. S2e). These results suggest that the availability of silicic acid affected little the decreases in relative diatom contribution to Chl *a* biomass. Larger diatoms could contribute to efficient transfer of energy and organic compounds to higher trophic levels because they would create a shorter food chain compared with nano- and pico-sized phytoplankton (Michaels and Silver, 1988). Because diatoms form a large part of phytoplankton biomass in the Bering Sea basin (Suzuki et al., 2002; Takahashi et al., 2002), the decrease in the relative contribution of diatoms with increasing CO_2 could reduce the energy transferred from the primary producers to the higher trophic levels.

The decreases in Fuco growth and relative contribution of diatoms were larger in the control bottles than those in the Fe-added treatments (Figs. 1 and 2), suggesting that the negative effect of CO_2 enrichment was greater in the Fe-limited conditions. These results are consistent with Sugie et al. (2013) and Yoshimura et al. (2014), who observed significant decreases in diatom carbon biomass and particulate organic carbon (POC) production under high CO_2 levels in the control treatments, whereas those were insignificantly changed in the Fe-added treatments. Sugie et al. (2013) indicated that the Fe limitations for phytoplankton in the control bottles were enhanced at high CO_2 levels, likely due to the reduction of Fe bioavailability as reported in Shi et al. (2010). The combined effects of CO_2 and Fe availability were also tested in a diatom-dominated phytoplankton community in the Southern Ocean (Hoppe et al., 2013). In their study, net primary productivity in seawater decreased with increased pCO_2 levels in the Fe-depleted treatments but not in the Fe-enriched treatments. These studies indicate that an interactive effect of CO_2 enrichment and Fe limitation could occur in the diatom-dominated natural phytoplankton assemblages in the HNLC region.

4.2 *rbcL* expression in diatoms

A significant correlation between diatom *rbcL* copies per liter and Fuco concentration was found in this study (Fig. 3), suggesting the usefulness of the *rbcL* gene fragment as a proxy for diatoms. In addition, the cDNA sequences obtained from cloning were dominated by the diatom-derived *rbcL* gene (Fig. 6). These results indicate that the *rbcL* primers used successfully and selectively amplified the *rbcL* gene of diatoms. Suzuki et al. (2011) showed that Fuco concentration significantly correlated with diatom carbon biomass in the subarctic Pacific. Furthermore, Matsuda et al. (2011) showed that the number of *rbcL* gene per cell varies among diatom species, and it was positively correlated with cell size. Therefore, we concluded that the *rbcL* gene could serve as a potential molecular marker for diatom biomass.

The transcript abundance of the diatom-specific *rbcL* gene decreased with elevated CO_2 levels in both the control and Fe-added treatments (Fig. 4). Because RuBisCO expression is primarily controlled at the transcriptional level in the natural phytoplankton community (Xu and Tabita, 1996; Wawrik et al., 2002), our results suggest that increased CO_2 levels could reduce the amount of RuBisCO in diatoms. It should be noted that significant decreases in *rbcL* expression with increased CO_2 levels were observed on days 2 and 3, when macronutrients still remained (Fig. S2). This indicates that the downregulation of *rbcL* expression in diatoms was probably caused by the increase in CO_2 availability. It has been shown that some land plants can increase their nitrogen utilization efficiency under elevated CO_2 levels by reducing the investment of nitrogen in RuBisCO (Curtis et al., 1989; Makino et al., 2003). Losh et al. (2012, 2013) also demonstrated a decreased RuBisCO contribution to the total protein in the California Current phytoplankton community with an increase in CO_2 level. Because a decrease in the expression of RuBisCO can result in a reduction of the potential capacity for carbon fixation in the natural environment (John et al., 2007b), our results indicate that an increase in CO_2 levels could have a negative impact on photosynthetic carbon fixation for diatoms in the study area. Recently, Gontero and Salvucci (2014) pointed out that RuBisCO activase plays a key role in the modification of RuBisCO activity, and consequently in the capacity of carbon fixation, although the occurrence of RuBisCO activase in diatoms is not well understood. Further studies must be needed for better understanding of the impacts of elevated CO_2 on photosynthetic physiology in diatoms.

The negative effects of increasing CO_2 on diatom biomass were not severe in the Fe-added bottles relative to Fe-limited control bottles (Fig. 1a and b), whereas *rbcL* transcripts decreased with increased CO_2 regardless of Fe availability (Fig. 4). This suggests that the diatoms could overcome the

decrease in RuBisCO activity in the Fe-added treatments. According to our cloning data (Fig. 6), a shift in phylogenetic composition of the diatoms actively transcribed *rbcL* was observed in the Fe-added bottles. In addition, F_v/F_m values increased significantly with Fe enrichment in our incubation experiments (Sugie et al., 2013), indicating an increase in the photochemical quantum efficiency of photosystem II for the diatoms. Therefore, the photosystem II activity might compensate for the decrease in RuBisCO expression under Fe-replete conditions.

It is generally recognized that phytoplankton autonomously regulate the transcription of the *rbcL* gene in response to environmental conditions such as light and nutrient availability (Pichard et al., 1996; Granum et al., 2009; John et al., 2010). However, the mechanisms controlling the transcription of RuBisCO operon in diatoms are largely unknown. Recently, Minoda et al. (2010) showed that the red alga *Cyanidioschyzon merolae* increased *rbcL* transcription at high levels of NADPH, 3-phosphoglyceric acid (3-PGA), or ribulose-1,5-bisphosphate (RuBP) under the influence of the transcription factor Ycf30. In addition, it has been reported that regeneration of RuBP could be a limiting factor for the CBB cycle in high CO_2 conditions (von Caemmerer and Farquhar, 1981; Stitt, 1991; Onoda et al., 2005). Thus, one possible mechanism underlying the reduction of diatom *rbcL* transcripts observed in our study is related to a decrease in RuBP concentration in the chloroplasts due to the increase in CO_2 availability for diatoms. Because diatoms possess the same type of RuBisCO (Form ID) and gene homologs encoding the Ycf30 protein (i.e., *ycf30*) (Kowallik et al., 1995), they could control *rbcL* gene expression using the same mechanisms as *C. merolae*. Further studies using marine diatom cultures are required to obtain a better understanding of the physiological mechanisms controlling the expression of RuBisCO.

In our experiment, the rarefaction curves plateaued to some extent in all treatments (Fig. 5), indicating that the clone numbers screened from each library were statistically sufficient for further diversity analysis. Taxonomic compositions in the cDNA library were considerably different from those in the diatom carbon biomass revealed by microscopic analysis by Sugie et al. (2013), which were composed primarily by Chaetocerataceae. This implies that the predominant diatoms did not necessarily become transcriptionally active *rbcL* phylotypes in our experiment. In addition, because 16–42 % of the sequences were classified as unidentified diatoms or other eukaryotes, the primer set used in this study might be insufficient to estimate diatom composition at the family level.

The *rbcL* cDNA libraries in the Fe-added treatments differed significantly from the initial library, whereas those in the control treatments were not significantly different (Table 3), suggesting that the diatom blooms induced by Fe infusion were associated with the change in the relative contribution of *rbcL* expression in diatoms. For example, compared to the initial seawater, the relative contributions of Chaetocerataceae and unidentified centrics to the *rbcL* cDNA library increased markedly in the Fe-added bottles, whereas they remained minor components in the control bottles (Fig. 6). This indicates that the relative significance of the RuBisCO activity of these phylotypes could be increased by Fe enrichment. In addition, cDNA libraries were significantly different from each other at different CO_2 levels in the Fe-added bottles (Table 3). This indicates that the transcriptionally active phylotypes in diatoms could shift in response to an increase in the CO_2 level. On the other hand, the diversity indices for the diatom-specific *rbcL* cDNA sequences were not affected by CO_2 availability (Table 2). In addition, the highest chao1 (richness) value was observed in the C-600 treatment. These results suggest that the richness and/or diversity of diatom phylotypes actively transcribing the *rbcL* gene could have remained under elevated CO_2 levels.

5 Conclusions

The present study showed that an increase in CO_2 levels could have negative impacts on diatom biomass in the Bering Sea, especially under Fe-limited conditions. Because diatoms play pivotal roles in carbon sequestration and food webs in the Bering Sea (Springer et al., 1996; Takahashi et al., 2002), our results indicate that ocean acidification might alter the biogeochemical processes and ecological dynamics in the study area. Although the present results cannot be extrapolated to other HNLC ecosystems due to differences in other environmental conditions, our findings suggest that the combined effects of CO_2 and other environmental factors such as Fe availability need to be examined for a better understanding of the potential impacts of ocean acidification on marine ecosystems.

We examined, for the first time, the relationships between CO_2 levels or Fe availability and RuBisCO expression of diatoms in the Bering Sea. Significant decreases in the *rbcL* expression of diatoms were observed at elevated CO_2 levels in both the Fe-limited and Fe-enriched treatments, suggesting that ocean acidification could reduce the primary productivity in the study area. Our results indicate that the amount of *rbcL* transcripts could be an important indicator to assess the physiological responses of RuBisCO activity in diatoms to environmental drivers. However, photosynthetic carbon fixation in diatoms can be controlled not only by RuBisCO activity, but also by other processes such as carbon concentrating mechanisms (CCMs) and/or RuBP regeneration (Rost et al., 2003; Onoda et al., 2005). More detailed studies on molecular mechanisms are required to clarify the physiological responses of the diatom community to CO_2 and Fe availability.

The Supplement related to this article is available online at doi:10.5194/bg-12-2247-2015-supplement.

Acknowledgements. We thank the captain, officers, and crew of the R/V *Hakuho Maru* for their great support and field assistance. We also thank J. Nishioka for Fe analysis. We show our appreciation to the editor and the three referees for providing constructive comments on the manuscript. This work was conducted within the framework of the Plankton Ecosystem Response to CO_2 Manipulation Study (PERCOM) and was partly supported by the grants from CRIEPI (no. 090313) and a Grant-in-Aid for Scientific Research (nos. 18067008, 22681004).

Edited by: E. Marañón

References

Badger, M. R., Whitney, S. M., Ludwig, M., Yellowlees, D. C., Leggat, W., and Price, G. D.: The diversity and co-evolution of RubisCO, plastids, pyrenoids, and chloroplast based CO_2-concentrating mechanisms in algae, Can. J. Bot., 76, 1052–1071, 1998.

Banse, K. and English, D. C.: Comparing phytoplankton seasonality in the eastern and western subarctic Pacific and the western Bering Sea, Prog. Oceanogr., 43, 235–288, 1999.

Boelen, P., van de Poll, W. H., van de Strate, H. J, Neven, I. A., Beardall, J., and Buma, A. G. J.: Neither elevated nor reduced CO_2 affects the photophysiological performance of the marine Antarctic diatom *Chaetoceros brevis*, J. Exp. Mar. Biol. Ecol., 406, 38–45, 2011.

Caldeira, K. and Wickett, M. E.: Anthropogenic carbon and ocean pH, Nature, 425, 365, 2003.

Chao, A.: Nonparametric estimation of the number of classes in a population, Scand. J. Stat., 11, 265–270, 1984.

Collins, S., Rost, B., and Rynearson, T. A.: Evolutionary potential of marine phytoplankton under ocean acidification, Evol. Appl., 7, 140–155, 2014.

Corredor, J. E., Wawrik, B., Paul, J. H., Tran, H., Kerkhof, L., Lopez, J. M, Dieppa, A., and Cardenas, O.: Geochemical rate-RNA integrated study: ribulose-1,5-bisphosphate carboxylase / oxygenase gene transcription and photosynthetic capacity of planktonic photoautotrophs, Appl. Environ. Microbiol., 70, 5459–5468, 2004.

Curtis, P. S., Drake, B. G., and Whigham, D. F.: Nitrogen and carbon dynamics in C_3 and C_4 marsh plants grown under elevated CO_2 in situ, Oecologia, 78, 297–301, 1989.

Edmond, J. M.: High precision determination of titration alkalinity and total carbon dioxide content of sea water by potentiometric titration, Deep-Sea Res., 17, 737–750, 1970.

Endo, H., Yoshimura, T., Kataoka, T., and Suzuki, K.: Effects of CO_2 and iron availability on phytoplankton and eubacterial community compositions in the northwest subarctic Pacific, J. Exp. Mar. Biol. Ecol., 439, 160–175, 2013.

Engel, A., Schulz, K. G., Riebesell, U., Bellerby, R., Delille, B., and Schartau, M.: Effects of CO_2 on particle size distribution and phytoplankton abundance during a mesocosm bloom experiment (PeECE II), Biogeosciences, 5, 509–521, doi:10.5194/bg-5-509-2008, 2008.

Feng, Y., Hare, C. E., Leblanc, K., Rose, J. M., Zhang, Y., DiTullio, G. R., Lee, P. A., Wilhelm, S. W., Rowe, J. M., Sun, J., Nemcek, N., Gueguen, C., Passow, U., Benner, I., Brown, C., and Hutchins, D. A.: Effects of increased pCO_2 and temperature on the North Atlantic spring bloom. I. The phytoplankton community and biogeochemical response, Mar. Ecol. Prog. Ser. 388, 13–25, 2009.

Feng, Y., Hare, C. E., Rose, J. M., Handy, S. M., DiTullio, G. R., Lee, P. A., Smith Jr, W. O., Peloquin, J., Tozzi, S., Sun, J., Zhang, Y., Dunbar, R. B., Long, M. C., Sohst, B., Lohan, M., and Hutchins, D. A.: Interactive effects of iron, irradiance and CO_2 on Ross Sea phytoplankton, Deep-Sea Res. I, 57, 368–383, 2010.

Gontero, B. and Salvucci, M. E.: Regulation of photosynthetic carbon metabolism in aquatic and terrestrial organisms by Rubisco activase, redox-modulation and CP12, Aquat. Bot., 118, 14–23, 2014.

Granum, E., Roberts, K., Raven, J. A., and Leegood, R. C.: Primary carbon and nitrogen metabolic gene expression in the diatom *Thalassiosira pseudonana* (Bacillariophyceae): Diel periodicity and effects of inorganic carbon and nitrogen, J. Phycol., 45, 1083–1092, 2009.

Hare, C. E., Leblanc, K., DiTullio, G. R., Kudela, R. M., Zhang, Y., Lee, P. A., Riseman, S., and Hutchins, D. A.: Consequences of increased temperature and CO_2 for phytoplankton community structure in the Bering Sea, Mar. Ecol. Prog. Ser., 352, 9–16, 2007.

Harrison, P. J., Conway, H. L., Holmes, R. W., and Davis, C. O.: Marine diatoms grown in chemostats under silicate or ammonium limitation. III. Cellular chemical composition and morphology of *Chaetoceros debilis*, *Skeletonema costatum*, and *Thalassiosira gravida*, Mar. Biol., 43, 19–31, 1977.

Hoppe, C. J., Hassler, C. S., Payne, C. D., Tortell, P. D., Rost, B., and Trimborn, S.: Iron limitation modulates ocean acidification effects on Southern Ocean phytoplankton communities, PloS One, 8, e79890, doi:10.1371/journal.pone.0079890, 2013.

Ihnken, S., Roberts, S., and Beardall, J.: Differential responses of growth and photosynthesis in the marine diatom *Chaetoceros muelleri* to CO_2 and light availability, Phycologia, 50, 182–193, 2011.

Jeffrey, S. W. and Wright, S. W.: Photosynthetic pigments in the Haptophyta, in: The Haptophyte algae, edited by: Green, J. C. and Leadbeater, B. S. C., Carendon Press, Oxford, 111–132, 1994.

Jiang, Y., Yin, K., Berges, J. A., and Harrison, P. J.: Effects of silicate resupply to silicate-deprived *Thalassiosira weissflogii* (Bacillariophyceae) in stationary or senescent phase: short-term patterns of growth and cell death, J. Phycol., 50, 602–606, 2014

John, D. E., Patterson, S. S., and Paul, J. H.: Phytoplankton group specific quantitative polymerase chain reaction assays for RuBisCO mRNA transcripts in seawater, Mar. Biotechnol., 9, 747–759, 2007a.

John, D. E., Wang, Z. A., Liu, X. W., Byrne, R. H., Corredor, J. E., Lopez, J. M., Cabrera, A., Bronk, D. A., Tabita, F. R., and Paul, J. H.: Phytoplankton carbon fixation gene (RuBisCO) transcripts and air-sea CO_2 flux in the Mississippi River plume, ISME J., 1, 517–531, 2007b.

John, D. E., Jose, López-Díaz, J. M., Cabrera, A., Santiago, N. A., Corredor, J. E., Bronk, D. A., and Paul, J. H.: A day in the life in the dynamic marine environment: how nutrients shape diel patterns of phytoplankton photosynthesis and carbon fixation gene

expression in the Mississippi and Orinoco River plumes, Hydrobiologia, 679, 155–173, 2010.

Kim, J.-M., Lee, K., Shin, K., Kang, J. -H., Lee, H. -W., Kim, M., Jang, P.-G., and Jang, M.-C.: The effect of seawater CO_2 concentration on growth of the natural phytoplankton assemblage in a controlled mesocosm experiment, Limnol. Oceanogr., 51, 1629–1636, 2006.

Kowallik, K. V., Stoebe, B., Schaffran, I., KrothPancic, P., and Freier, U.: The chloroplast genome of a chlorophyll $a + c$-containing alga, Odontella sinensis, Plant Mol. Biol. Rep., 13, 336–342, 1995.

Latasa, M.: Improving estimations of phytoplankton class abundances using CHEMTAX, Mar. Ecol. Prog. Ser., 329, 13–21, 2007.

Lewis, E. and Wallance, D. W. R.: Program developed for CO_2 system calculations. ORNL/CDIAC-105. Carbon dioxide information analysis center, Oak Ridge National Laboratory, US Department of Energy, Oak Ridge, Tennessee, 1998.

Losh, J. L., Morel, F. M. M., and Hopkinson, B. M.: Modest increase in the C:N ratio of N-limited phytoplankton in the California Current in response to high CO_2, Mar. Ecol. Prog. Ser., 468, 31–42, 2012.

Losh, J. L., Young, J. N., and Morel, F. M.: Rubisco is a small fraction of total protein in marine phytoplankton, New Phytol., 198, 52–58, 2013.

Luu-The, V., Paquet, N., Calvo, E., and Cumps, J.: Improved real-time RT-PCR method for high-throughput measurements using second derivative calculation and double correction, Biotechniques, 38, 287–293, 2005.

Mackey, M. D., Mackey, D. J., Higgins, H. W., and Wright, S. W.: CHEMTAX-a program for estimating class abundances from chemical markers: application to HPLC measurements of phytoplankton, Mar. Ecol. Prog. Ser., 144, 265–283, 1996.

Mackinder, L., Wheeler, G., Schroeder, D., Riebesell, U., and Brownlee, C.: Molecular mechanisms underlying calcification in coccolithophores, Geomicrobiology, 27, 585–595, 2010.

Makino, A., Sakuma, H., Sudo, E., and Mae, T.: Differences between Maize and Rice in N-use efficiency for photosynthesis and protein allocation, Plant Cell Physiol., 44, 952–956, 2003.

Matsuda, Y., Nakajima, K., and Tachibana, M.: Recent progresses on the genetic basis of the regulation of CO_2 acquisition systems in response to CO_2 concentration, Photosynth. Res., 109, 191–203, 2011.

Meakin, N. G. and Wyman, M.: Rapid shifts in picoeukaryote community structure in response to ocean acidification, ISME J., 5, 1397–1405, 2011.

Meehl, G. A., Stocker, T. F., Collins, W. D., Friedlingsten, P., Gaye, A. T., Gregory, J. M., Kitoh, A., Knutti, R., Murphy, J. M., Noda, A., Raper, S. C. B., Watterson, I. G., Weaver, A. J., and Zhao, Z. -C.: Global Climate Projections, in: Climate Change 2007 The Physical Science Basis, Contribution of Working Group I to the Fourth Assessment Report of the Intergovernmental Panel on Climate Change, edited by: Solomon, S., Qin, D., Manning, M., Chen, Z., Marquis, M., Averyt, K., Tignor, M. M. B., and Miller, H. L., Cambridge University Press, United Kingdom and New York, 2007.

Michaels, A. F. and Silver, M. W.: Primary Production, sinking fluxes and the microbial food web, Deep-Sea Res., 35, 473–490, 1988.

Minoda, A., Weber, A. P. M., Tanaka, K., and Miyagishima, S.: Nucleus-independent control of the Rubisco operon by the plastid-encoded transcription factor Ycf30 in the red alga *Cyanidioschyzon merolae*, Plant Physiol., 154, 1532–1540, 2010.

Obata, H., Karatani, H., and Nakayama, E.: Automated determination of iron in seawater by chelating resin concentration and chemiluminescence detection, Anal. Chem., 65, 1524–1528, 1993.

Ondrusek, M. E., Bidigare, R. R., Sweet, S. T, Defreitas, D. A., and Brooks, J. M.: Distribution of phytoplankton pigments in the North Pacific Ocean in relation to physical and optical variability, Deep-Sea Res., 38, 243–266, 1991.

Onoda, Y., Hikosaka, K., and Hirose, T.: Seasonal change in the balance between capacities of RuBP carboxylation and RuBP regeneration affects CO_2 response of photosynthesis in *Polygonum cuspidatum*, J. Exp. Bot., 56, 755–763, 2005.

Pearson, P. N. and Palmer, M. R.: Atmospheric carbon dioxide concentration over the past 60 million years, Nature, 406, 659–699, 2000.

Pichard, S. L., Campbell, L., Kang, J. B., Tabita, F. R., and Paul, J. H.: Regulation of ribulose bisphosphate carboxylase gene expression in natural phytoplankton communities 1. Diel rhythms, Mar. Ecol. Prog. Ser., 139, 257–265, 1996.

Raven, J., Caldeira, K., Elderfield, H., Hoegh-Guldberg, O., Liss, P., Riebesell, U., Shepherd, J., Turley, C., and Watson, A.: Ocean acidification due to increasing atmospheric carbon dioxide, The Royal Society policy document 12/05, Cardiff: Clyvedon Press, 2005.

Riebesell, U. and Tortell, P. D.: Effects of ocean acidification on pelagic organisms and ecosystems, in: Ocean acidification, edited by: Gattuso, J.-P., and Hansson, L., Oxford University Press, New York, 83–98, 2011.

Riebesell, U., Schulz, K. G., Bellerby, R. G. J., Botros, M., Fritsche, P., Meyerhöfer, M., Neill, C., Nondal, G., Oschlies, A., Wohlers, J., and Zöllner, E.: Enhanced biological carbon consumption in a high CO_2 ocean, Nature, 450, 545–548, 2007.

Rost, B., Riebesell, U., Burkhardt, S., and Sültemeyer, D.: Carbon acquisition of bloom forming marine phytoplankton, Limnol. Oceanogr., 48, 55–67, 2003.

Sabine, C. L., Feely, R. A., Gruber, N., Key, R. M., Lee, K., Bullister, J. L., Wanninkhof, R., Wong, C. S., Wallace, D. W. R., Tilbrook, B., Millero, F. J., Peng, T.-H., Kozyr, A., Ono, T., and Rios, A. F.: The oceanic sink for anthropogenic CO_2, Science, 305, 367–371, 2004.

Schloss, P. D., Westcott, S. L., Ryabin, T., Hall, J. R., Hartmann, M., Hollister, E. B., Lesniewski, R. A., Oakley, B. B., Parks, D. H., Robinson, C. J., Sahl, J. W., Stres, B., Thallinger, G. G., Van Horn, D. J., and Weber, C. F.: Introducing mothur: open-source, platform-independent, community-supported software for describing and comparing microbial communities, Appl. Environ. Microbiol., 75, 7537–7541, 2009.

Schoemann, V., Becquevort, S., Stefels, J., Rousseau, V., and Lancelot, C.: Phaeocystis blooms in the global ocean and their controlling mechanisms: a review, J. Sea Res., 53, 43–66, 2005.

Shannon, C. E.: A mathematical theory of communication, AT&T Teck. J., 27, 379–423, 1948.

Shi, D., Xu, Y., Hopkinson, B. M., and Morel, F. M. M.: Effect of ocean acidification on iron availability to marine phytoplankton, Science, 327, 676–679, 2010.

Simpson, E. H.: Measurement of diversity, Nature, 163, 688, 1949.

Singleton, D. R., Furlong, M. A., Rathbun, S. L., and Whitman, W. B.: Quantitative comparisons of 16S rRNA gene sequence libraries from environmental samples, Appl. Environ. Microbiol., 67, 4374–4376, 2001.

Smith, C. J., Nedwell, D. B., Dong, L. F., and Osborn, A. M.: Evaluation of quantitative polymerase chain reaction-based approaches for determining gene copy and gene transcript number in environmental samples, Environ. Microbiol., 8, 804–815, 2006.

Springer, A. M., McRoy, C. P., and Flint, M. V.: The Bering Sea Green Belt: shelf-edge processes and ecosystem production, Fish. Oceanogr., 5, 205–223, 1996.

Stitt, M.: Rising CO_2 levels and their potential significance for carbon flow in photosynthetic cells, Plant Cell Environ., 14, 741–762, 1991.

Sugie, K., Endo, H., Suzuki, K., Nishioka, J., Kiyosawa, H., and Yoshimura, T.: Synergistic effects of pCO_2 and iron availability on nutrient consumption ratio of the Bering Sea phytoplankton community, Biogeosciences, 10, 6309–6321, doi:10.5194/bg-10-6309-2013, 2013.

Suzuki, K., Minami, C., Liu, H., and Saino, T.: Temporal and spatial patterns of chemotaxonomic algal pigments in the subarctic Pacific and the Bering Sea during the early summer of 1999, Deep-Sea Res. II, 49, 5685–5704, 2002.

Suzuki, K., Kuwata, A., Yoshie, N., Shibata, A., Kawanobe, K., and Saito, H.: Population dynamics of phytoplankton, heterotrophic bacteria, and viruses during the spring bloom in the western subarctic Pacific, Deep-Sea Res. I, 58, 575–589, 2011.

Takahashi, K., Fujitani, N., and Yanada, M.: Long term monitoring of particle fluxes in the Bering Sea and the central subarctic Pacific Ocean, 1990–2000, Prog. Oceanogr., 55, 95–112, 2002.

Tortell, P. D., DiTullio, G. R., Sigman, D. M., and Morel, F. M. M.: CO_2 effects on taxonomic composition and nutrient utilization in an Equatorial Pacific Phytoplankton assemblage, Mar. Ecol. Prog. Ser., 236, 37–43, 2002.

Tortell, P. D., Payne, C. D., Li, Y., Trimborn, S., Rost, B., Smith, W. O., Riesselan, C., Dunbar, R. B., Sedwick, P., and DiTullio, G. R.: CO_2 sensitivity of Southern Ocean phytoplankton, Geophys. Res. Lett., 35, L04605, doi:10.1029/2007GL032583, 2008.

Trimborn, S., Brenneis, T., Sweet, E., and Rost, B.: Sensitivity of Antarctic phytoplankton species to ocean acidification: Growth, carbon acquisition, and species interaction, Limnol. Oceanogr., 58, 997–1007, 2013.

Von Caemmerer, S. V. and Farquhar, G. D.: Some relationships between the biochemistry of photosynthesis and the gas exchange of leaves, Planta, 153, 376–387, 1981.

Wawrik, B., Paul, J. H., and Tabita, F. R.: Real-time PCR quantification of *rbcL* (ribulose-1,5-bisphosphate carboxylase / oxygenase) mRNA in diatoms and pelagophytes, Appl. Environ. Microbiol., 68, 3771–3779, 2002.

Welschmeyer, N. A.: Fluorometric analysis of chlorophyll *a* in the presence of chlorophyll *b* and pheopigments, Limnol. Oceanogr., 39, 1985–1992, 1994.

WMO: Greenhouse gas bulletin: The state of greenhouse gases in the atmosphere based on global observations through 2012, World Meteorological Organization, Geneva, Switzerland, ISSN 2078–0796, 2013.

Wright, S. W. and van den Enden, R. L.: Phytoplankton community structure and stocks in the east Antarctic marginal ice zone (BROKE survey, January–March 1996) determined by CHEMTAX analysis of HPLC pigment signature, Deep-Sea Res. II, 47, 2363–2400, 2000.

Xu, H. H. and Tabita, F. R.: Ribulose-1.5-bisphosphate carboxylase / oxygenase gene expression and diversity of lake Erie planktonic microorganisms, Appl. Environ. Microbiol, 62, 1913–1921, 1996.

Yoshimura, T., Nishioka, J., Suzuki, K., Hattori, H., Kiyosawa, H., and Watanabe, Y.: Impacts of elevated CO_2 on organic carbon dynamics in nutrient depleted Okhotsk Sea surface waters, J. Exp. Mar. Biol. Ecol., 395, 191–198, 2010.

Yoshimura, T., Suzuki, K., Kiyosawa, H., Ono, T., Hattori, H., Kuma, K., and Nishioka, J.: Impacts of elevated CO_2 on particulate and dissolved organic matter production: Microcosm experiments using iron deficient plankton communities in open subarctic waters, J. Oceanogr., 69, 601–618, 2013.

Yoshimura, T., Sugie, K., Endo, H., Suzuki, K., Nishioka, J., and Ono, T.: Organic matter production response to CO_2 increase in open subarctic plankton communities: Comparison of six microcosm experiments under iron-limited and-enriched bloom conditions, Deep-Sea Res. I, 94, 1–14, 2014.